Unsteady MHD flow and heat transfer near stagnation point over a stretching/shrinking sheet in porous medium filled with a nanofluid

Sadegh Khalili[a)], Saeed Dinarvand[b)†], Reza Hosseini[b)], Hossein Tamim[c)], and Ioan Pop[d)]

[a)] *Young Researchers and Elite Club, Saveh Branch, Islamic Azad University, Saveh, Iran*
[b)] *Mechanical Engineering Department, Amirkabir University of Technology, 424 Hafez Avenue, Tehran, Iran*
[c)] *Department of Mechanical Engineering, Saveh Branch, Islamic Azad University, Saveh, Iran*
[d)] *Department of Mathematics, Babeş-Bolyai University, 400084 Cluj-Napoca, Romania*

(Received 19 June 2013; revised manuscript received 13 October 2013; published online 20 February 2014)

In this article, the unsteady magnetohydrodynamic (MHD) stagnation point flow and heat transfer of a nanofluid over a stretching/shrinking sheet is investigated numerically. The similarity solution is used to reduce the governing system of partial differential equations to a set of nonlinear ordinary differential equations which are then solved numerically using the fourth-order Runge–Kutta method with shooting technique. The ambient fluid velocity, stretching/shrinking velocity of sheet, and the wall temperature are assumed to vary linearly with the distance from the stagnation point. To investigate the influence of various pertinent parameters, graphical results for the local Nusselt number, the skin friction coefficient, velocity profile, and temperature profile are presented for different values of the governing parameters for three types of nanoparticles, namely copper, alumina, and titania in the water-based fluid. It is found that the dual solution exists for the decelerating flow. Numerical results show that the extent of the dual solution domain increases with the increases of velocity ratio, magnetic parameter, and permeability parameter whereas it remains constant as the value of solid volume fraction of nanoparticles changes. Also, it is found that permeability parameter has a greater effect on the flow and heat transfer of a nanofluid than the magnetic parameter.

Keywords: nanofluid, Navier–Stokes equations, MHD, dual solutions, porous media

PACS: 82.70.–y, 47.10.Ad, 52.30.Cv, 02.60.Cb **DOI:** 10.1088/1674-1056/23/4/048203

1. Introduction

Stagnation flow occurs whenever a flow impinges onto a solid object and is of considerable technical relevance, for example in turbo-machinery, flows over the submarines and oil ships or the leading edge of an aerofoil. In the stagnation region, pressure is at its maximum value and the highest rates of heat transfer and mass deposition occur. The unsteady boundary layer was studied initially by Moore[1] and Lin.[2] The flow and heat transfer characteristics of such an unsteady process in the gradual switch-off process were investigated both analytically and numerically in the boundary layer approximation, assuming a linear variation of the steady stretching velocity with the longitudinal coordinate and an inverse linear law for its decrease with time. Wang[3] studied the concept of the flow of liquid film on an unsteady stretching surface. Bachok *et al.*[4] presented a similarity solution for the unsteady flow and heat transfer of a nanofluid over a permeable stretching/shrinking sheet and found that dual solutions exist for both stretching and shrinking cases. Suali *et al.*[5] studied the effects of suction and injection into the boundary layer on the unsteady stagnation point flow over a stretching/shrinking sheet. Fang *et al.*[6] analyzed the effect of unsteadiness on the viscous flow over an expanding stretching cylinder. The boundary layer flow due to a stretching surface is important in extrusion processes such as metal sheet extrusion, polymer extrusion, and other industrial processes such as hot rolling, drawing, crystal growth, and paper production and food production. In elastic materials under constant strain, stretching velocity is linearly increasing with the increase of distance from the leading edge. The unsteady flow over a continuously shrinking surface with wall mass suction in a water-based nanofluid containing different types of nanoparticles was investigated numerically by Rohni *et al.*[7] Shahzad *et al.*[8] considered a nonlinear stretching sheet within a porous medium. Wang[9] studied the steady two-dimensional (2D) and axisymmetric stagnation point flow with heat transfer over a shrinking sheet and found that there is a critical value of shrinking rate and solutions do not exist for the larger values of shrinking rates. The steady three-dimensional (3D) stagnation point flow of a nanofluid past a circular cylinder with sinusoidal radius variation was studied by Dinarvand *et al.*[10]

The thermal conductivity of fluids has a significant influence on the heat transfer coefficient between the medium and surface. The poor heat transfer properties of regular fluids such as oil, water, and ethylene glycol, compared with most solids are a primary problem for the high compactness and effectiveness of heat exchangers. On the other hand, due to the rapid development of modern technology, recent microelectromechanical systems (MEMS) generate a huge amount of heat, which affects the normal performances of the devices and re-

†Corresponding author. E-mail: dinarvand@yahoo.com; dinarvand@aut.ac.ir
© 2014 Chinese Physical Society and IOP Publishing Ltd

duces reliability. Therefore, an efficient cooling system is one of the most important problems in designing MEMS components. A novel technique to improve the thermal conductivity is to incorporate nanoparticles in the base fluid (See Kamali and Binesh[11]). Nanofluid is a new class of nanotechnology-based heat transfer fluids engineered by dispersing nanometer-scale solid particles with typical length scales of the order of 1 nm to 100 nm in traditional heat transfer fluids. The presence of the nanoparticles in a fluid increases the effective thermal conductivity of the fluid and consequently enhances the heat transfer characteristics. This fact has attracted many researchers such as Choi,[12] Khanafer *et al.*,[13] Tiwari and Das,[14] Oztop and Abu-Nada,[15] Zhou and Gao,[16] Tamim *et al.*,[17] Dinarvand *et al.*,[18] Khalili *et al.*,[19] etc. The comprehensive references on nanofluids can be found in the book by Das *et al.*[20] and in the review papers by Kakaç and Pramuanjaroenkij,[21] Eagen *et al.*,[22] Lee *et al.*,[23] and Fan and Wang.[24]

The study of magnetohydrodynamic (MHD) flow has aroused a great deal of research interest due to its importance in many engineering studies and industries, such as plasma studies, the boundary layer control in aerodynamics, MHD power generators, cooling of nuclear reactors, petroleum industries, and crystal growth. Takhar and Ram[25] have studied MHD forced and free convection flow through a porous medium in the presence of a uniform transverse magnetic field. Raptis *et al.*[26] have analyzed hydromagnetic free convection flow through a porous medium between two parallel plates. Fang and Zhang[27] found a closed-form exact solution for 2D MHD flow over a porous shrinking sheet subjected to wall-mass transfer. Fang *et al.*[28] considered the effect of velocity slip on MHD flow over a permeable shrinking sheet. They concluded that the velocity slip at the shrinking sheet can greatly affect the velocity distribution and drag forces on the wall. Recently, Khalili *et al.*[29] studied the MHD stagnation point flow toward the stretching/shrinking permeable plate in a porous medium filled with a nanofluid. Convection heat transfer and fluid flow through a porous medium have many important applications in geophysical fields such as geothermal and petroleum resources. Solid matrix heat exchanges, drying of porous solids, thermal insulation and enhanced oil recovery are some of industrial applications of boundary layer problems in a porous medium. Several excellent books by Nakayama,[30] Nield and Bejan[31] and Ingham and Pop[32] have appeared recently dealing with this area, which review the present understanding of the basic mechanisms involved as well as showing how these influence the practical applications.

The objective of this paper is to present a detailed study on the development of the unsteady 2D boundary layer flow and heat transfer of a viscous nanofluid in the region of the stagnation point on a stretching/shrinking sheet in a porous medium. A transverse magnetic field is applied and the fluid is assumed to be incompressible. Using a similarity transformation, the Navier–Stokes equations are reduced to a set of nonlinear ordinary differential equations. The resulting nonlinear system is solved numerically for three different types of nanofluids using the fourth-order Runge–Kutta method with shooting technique. The results obtained are then compared with those of Suali *et al.*,[5] Wang,[9] and Bachok *et al.*[33] to support their validity. The literature survey reveals that there are regions of unique solutions for accelerating flows and dual solutions for decelerating flows. We restrict our study to a common Prandtl number for nanofluids, taking $Pr = 6.2$. For other values of Pr, we expect to have qualitatively similar results.

2. Nanofluid flow and mathematical formulation

Consider a 2D laminar stagnation point flow of an electrically conducting Newtonian nanofluid over a stretching/shrinking sheet in a porous medium as shown in Fig. 1. Cartesian coordinates x and y are taken with the origin o at the stagnation point, and are defined such that the x axis is measured along the stretching/shrinking sheet and the y axis is measured normal to it.

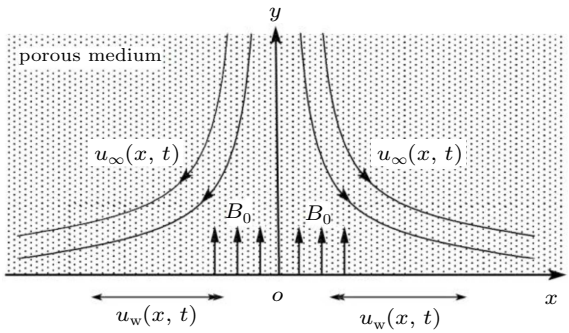


Fig. 1. Schematic plot of the problem and coordinate system.

It is assumed that the velocity of the inviscid flow is given by $u_\infty = ax/(1-ct)$ and the sheet is stretched with velocity $u_w = bx/(1-ct)$ where $a > 0$ is the strength of the stagnation flow, b is the ratio of stretching/shrinking velocity, with $b > 0$ for the stretching case and $b < 0$ for the shrinking case, and c is a constant. Let the surface temperature T_w be proportional to the distance from the stagnation point, i.e., $T_w(x) = T_\infty + T_0 x$ where T_0 is the characteristic temperature of the wall. It is assumed that the base fluid (i.e., water) and the nanoparticles are in thermal equilibrium and no slip occurs between them. The basic steady conservations of mass, momentum and energy equations for a nanofluid under a vertical magnetic field through a porous medium are

$$\frac{\partial u}{\partial x} + \frac{\partial v}{\partial y} = 0, \tag{1}$$

$$\frac{\partial u}{\partial t}+u\frac{\partial u}{\partial x}+v\frac{\partial u}{\partial y}=\frac{\partial u_\infty}{\partial t}+u_\infty\frac{\partial u_\infty}{\partial x}+\nu_{\rm nf}\frac{\partial^2 u}{\partial y^2}+\frac{\nu_{\rm nf}}{K}(u_\infty-u)+\frac{\sigma B_0^2}{\rho_{\rm nf}}(u_\infty-u), \quad (2)$$

$$\frac{\partial T}{\partial t}+u\frac{\partial T}{\partial x}+v\frac{\partial T}{\partial y}=\alpha_{\rm nf}\frac{\partial^2 T}{\partial y^2}, \quad (3)$$

with the initial and boundary conditions

$$\begin{aligned} &t<0: \quad u=v=0, \quad T=T_\infty \quad \text{for any } x,\ y,\\ &t\geq 0: \quad u=u_{\rm w}(x,t), \quad v=0, \quad T=T(x) \quad \text{at} \quad y=0,\\ &\qquad u\to u_\infty(x,t), \quad T\to T_\infty \quad \text{as} \quad y\to\infty, \end{aligned} \quad (4)$$

where u and v are the velocity components along the x axis and y axis, respectively, B_0 is the uniform magnetic field, σ is the electrical conductivity, $\nu_{\rm nf}$ is the kinematic viscosity of the nanofluid, $\rho_{\rm nf}$ is the density of the nanofluid, and $\alpha_{\rm nf}$ is the thermal diffusivity of the nanofluid, which are given by (see Oztop and Abu-Nada.[15])

$$\begin{aligned} &\frac{k_{\rm nf}}{k_{\rm f}}=\frac{(k_{\rm s}+2k_{\rm f})-2\phi(k_{\rm f}-k_{\rm s})}{(k_{\rm s}+2k_{\rm f})+\phi(k_{\rm f}-k_{\rm s})},\\ &(\rho C_{\rm p})_{\rm nf}=(1-\phi)(\rho C_{\rm p})_{\rm f}+\phi(\rho C_{\rm p})_{\rm s},\\ &\mu_{\rm nf}=\frac{\mu_{\rm f}}{(1-\phi)^{2.5}}, \quad \rho_{\rm nf}=(1-\phi)\rho_{\rm f}+\phi\rho_{\rm s},\\ &\nu_{\rm nf}=\frac{\mu_{\rm nf}}{\rho_{\rm nf}}, \quad \alpha_{\rm nf}=\frac{k_{\rm nf}}{(\rho C_{\rm p})_{\rm nf}}. \end{aligned} \quad (5)$$

Here ϕ is the solid volume fraction of the nanofluid, $\rho_{\rm f}$ is the density of the base fluid and $\rho_{\rm s}$ is the density of the solid particle. It is worth mentioning that the viscosity of the nanofluid $\mu_{\rm nf}$ can be approximated as viscosity of a base fluid $\mu_{\rm f}$ containing dilute suspension of fine spherical particles and its expression has been given by Brinkman.[34] In order to obtain similarity solutions of Eqs. (1)–(3) with the boundary conditions (4), we introduce the following similarity:

$$\begin{aligned} &\psi=\left(\frac{a\nu_{\rm f}}{1-ct}\right)^{1/2}xf(\eta), \quad \eta=\left(\frac{a}{\nu_{\rm f}(1-ct)}\right)^{1/2}y,\\ &\theta(\eta)=\frac{T-T_\infty}{T_{\rm w}-T_\infty}, \end{aligned} \quad (6)$$

where ψ is the stream function defined as $u=\partial\psi/\partial y$ and $v=-\partial\psi/\partial x$, which identically satisfy Eq. (1). Using the non-dimensional variables in Eqs. (6), equations (2) and (3) reduce to the following ordinary differential equations:

$$f'''+\{(1-\varphi)^{2.5}M+\kappa\}(1-f')+(1-\varphi)^{2.5}\left(1-\varphi+\varphi\frac{\rho_{\rm s}}{\rho_{\rm f}}\right)\times\left\{ff''+1-f'^2+\xi\left(1-f'-\frac{1}{2}\eta f''\right)\right\}=0, \quad (7)$$

$$\frac{k_{\rm nf}}{k_{\rm f}}\theta''+Pr\left((1-\varphi)+\varphi\frac{(\rho C_{\rm p})_{\rm s}}{(\rho C_{\rm p})_{\rm f}}\right)\left\{f\theta'-f'\theta-\frac{\xi}{2}\eta\theta'\right\}=0, \quad (8)$$

where κ is the permeability parameter of the medium, M is the magnetic parameter, $\xi=c/a$ is unsteadiness parameter, with $\xi>0$ and $\xi<0$ for flows with positive and negative local acceleration, respectively, while $\xi=0$ corresponds to steady state flow, $Pr=\nu_{\rm f}/\alpha_{\rm f}$ is the Prandtl number of the base fluid, and primes denote differentiation with respect to η. The boundary conditions (4) become

$$\begin{aligned} &f(0)=0, \quad f'(0)=b/a=\varepsilon, \quad \theta(0)=1,\\ &f'(\eta)\to 1, \quad \theta(\eta)\to 0 \quad \text{as} \quad \eta\to\infty. \end{aligned} \quad (9)$$

The velocity ratio parameter ε is defined as the ratio between stretching rate of the sheet and strength of the free stream. $\varepsilon>0$, $\varepsilon<0$, and $\varepsilon=1$ correspond to stretching sheet, shrinking sheet, and the flow with no boundary layer ($u_{\rm w}=u_\infty$), respectively, while $\varepsilon=0$ is the planar stagnation flow towards a stationary sheet. The skin friction coefficient $C_{\rm f}$ and the local Nusselt number Nu_x are the physical quantities of interest which are defined as

$$C_{\rm f}=\frac{\tau_{\rm w}}{\rho_{\rm f}u_\infty^2}, \quad Nu_x=\frac{xq_{\rm w}}{k_{\rm f}(T_{\rm w}-T_\infty)}, \quad (10)$$

where $\tau_{\rm w}$ is the surface shear stress and $q_{\rm w}$ is the surface heat flux which are given, respectively, by

$$\tau_{\rm w}=\mu_{\rm nf}\left(\frac{\partial u}{\partial y}\right)_{y=0}, \quad q_{\rm w}=-k_{\rm nf}\left(\frac{\partial T}{\partial y}\right)_{y=0}. \quad (11)$$

Substituting Eqs. (6) into Eqs. (10) and (11) we obtain

$$\begin{aligned} &C_{\rm f}(Re_x)^{1/2}=\frac{1}{(1-\phi)^{2.5}}f''(0),\\ &Nu_x(Re_x)^{-1/2}=-\frac{k_{\rm nf}}{k_{\rm f}}\theta'(0), \end{aligned} \quad (12)$$

where $Re_x=u_\infty x/\nu_{\rm f}$ is the local Reynolds number.

3. Results and discussion

The system of nonlinear ordinary differential equations (7) and (8) with the boundary conditions (9) are solved numerically using the fourth-order Runge–Kutta method with shooting technique and the results are reported for some values of the unsteadiness parameter ξ, nanoparticle volume fraction ϕ, permeability parameter κ, magnetic parameter M, and three different types of nanoparticles namely alumina, titania, and copper with water serving as the base fluid. The thermophysical properties of the base fluid and the nanoparticles are listed in Table 1.

Table 1. Thermophysical properties of the base fluid and the nanoparticles (see Oztop and Abu-Nada[15]).

Physical properties	Base fluid (water)	Cu	Al_2O_3	TiO_2
$C_{\rm p}$/(J/kg·K)	4179	385	765	686.2
ρ/(kg/m^3)	997.1	8933	3970	4250
k/(W/mK)	0.613	400	40	8.9538
$\alpha\times10^{-7}$/(m^2/s)	1.47	1163.1	131.7	30.7

In order to verify the accuracy of the numerical results, the validity of the numerical code developed has been checked for limiting cases as follows. In the first case, we consider steady state flow of a regular fluid ($\phi = 0$) in nonporous medium ($\kappa = 0$) and in the absence of magnetic field ($M = 0$) then we compare our results with those given by Suali *et al.*[5] and Wang[9] for different values of velocity ratio ε (Table 2). In the next step, we compare our results with those given by Bachok *et al.*[33] for some values of ξ and different nanoparticles for $\varepsilon = \kappa = M = 0$ and constant wall temperature (Tables 3). The comparisons are found to be in excellent agreement, and thus give confidence that the numerical results obtained are accurate.

Table 2. The values of $f''(0)$ for some values of ε when $\kappa = M = 0$ for steady state flow of a regular fluid.

ε	Wang[9]		Suali *et al.*[5]		Present study	
	first solution	second solution	first solution	second solution	first solution	second solution
3			−4.4276545		−4.276541	
0.2	1.05113		1.051130		1.051130	
0.1	1.14656		1.146561		1.146561	
−0.1	1.30860		1.308602		1.308602	
−1	1.32882	0	1.328817	0	1.328817	0
−1.15	1.08223	0.116702	1.082232	0.116702	1.082231	0.116702

Table 3. The values of $f''(0)$ and $-\theta'(0)$ for some values of ξ when $\kappa = M = 0$ and $\phi = 0.1$ for different working fluids on stationary sheet with constant wall temperature.

ξ		Bachok *et al.*[33]			Present study		
		Cu	Al_2O_3	TiO_2	Cu	Al_2O_3	TiO_2
1	$f''(0)$	1.7604	1.4967	1.5128	1.760398	1.496695	1.512796
	$-\theta'(0)$	0.4681	0.4032	0.4076	0.468134	0.403245	0.407566
−1	$f''(0)$	1.0845	0.9221	0.9320	1.084530	0.922070	0.931990
		[−1.1573]	[−0.9839]	[−0.9945]	[−1.157288]	[−0.983929]	[−0.994514]
	$-\theta'(0)$	1.4957	1.4663	1.4910	1.495740	1.466318	−1.490996
		[0.4638]	[0.4420]	[0.4491]	[0.463827]	[0.442016]	[0.449133]
−2	$f''(0)$	0.6499	0.5525	0.5585	0.649877	0.552527	0.558471
		[−1.9885]	[−1.6906]	[−1.7088]	[−1.988518]	[−1.690643]	[−1.708830]
	$-\theta'(0)$	1.8532	1.8335	1.8651	1.853218	1.833519	1.865106
		[1.3327]	[1.3565]	[1.3817]	[1.332676]	[1.356481]	[1.381657]

[ ]: second solution

The solution domain for Eqs. (7) and (8) with the boundary conditions (9) is illustrated in Figs. 2–7. We notice from these figures that there are regions of unique solution and regions of more than one solution and the solutions exist up to the critical value of ξ_{cr}. The dual solutions are obtained by setting different initial guesses for the values of $f''(0)$ and $\theta'(0)$, where all profiles satisfy the boundary conditions (9) with different shapes. Further, it should be mentioned that the upper branch solutions are stable and physically realizable, while the lower branch(s) solutions are not stable and not physically realizable. The procedure for showing this has been described by Postelnicu and Pop,[35] and Roşca and Pop.[36]

The variations of the skin friction coefficient $C_f Re_x^{1/2}$ and the Nusselt number $Nu_x Re_x^{-1/2}$ for different values of solid volume fraction ϕ with unsteadiness parameter ξ are shown in Fig. 2(a) and 2(b), respectively. It is seen that the critical unsteadiness parameter ξ_{cr} remains constant for different values of the solid volume fraction ϕ. We can see that the skin friction coefficient and the local Nusselt number increase as ϕ increases. Also, by changing the working nanofluid ξ_{cr} does not change (Fig. 3). The highest skin friction and heat transfer rate are achieved for Cu–water working fluid. This behavior of the local Nusselt number is similar to that reported by Oztop and Abu-Nada.[15] In addition, it is noted that the Cu nanoparticles have high values of thermal diffusivity; therefore, this reduces the temperature gradient which will affect the performance of Cu–water working fluid. As shown in Eq. (12), the skin friction coefficient is a function of ϕ and $f''(0)$ while the Nusselt number is a function of ϕ, $\theta'(0)$, and the type of nanoparticle. Therefore, we choose $C_f Re_x^{1/2}$ and $Nu_x Re_x^{-1/2}$ instead of $f''(0)$ and $-\theta'(0)$ for the vertical axes in figures that analyze the effect of the type of nanoparticle or solid volume fraction on the skin friction coefficient and the Nusselt number, respectively.

The effects of κ on $f''(0)$ and $-\theta'(0)$ are shown in Fig. 4. Figure 4(a) shows that as the absolute value of unsteadiness parameter increases, the first solution decreases from positive to negative values of $f''(0)$, which indicates that multiple regions exist for the velocity boundary layer. Also, it is seen that the extent of the dual solution domain increases as permeability parameter κ increases. The same behavior of solution is observed for different values of M (Fig. 5).

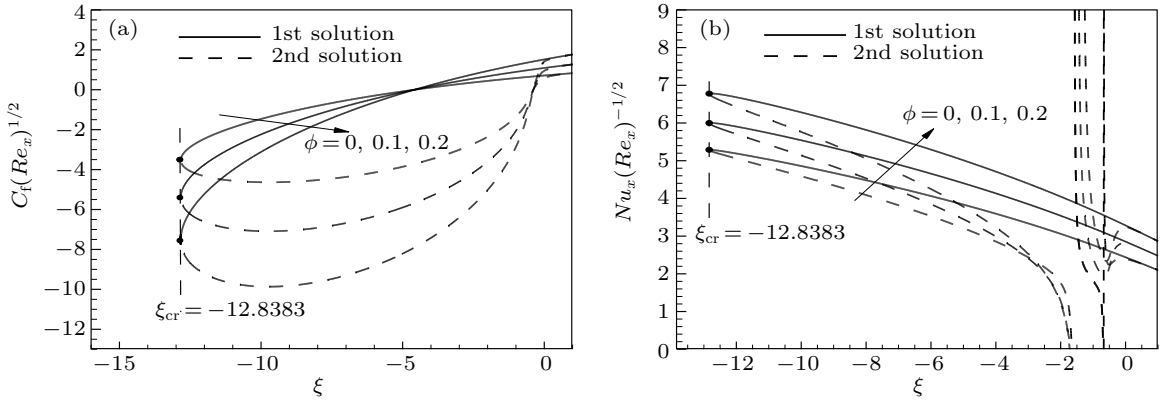


Fig. 2. $C_f Re_x^{1/2}$ (a) and $Nu_x Re_x^{-1/2}$ (b) as a function of ξ for different values of ϕ when $\kappa = M = 0$ and $\varepsilon = 0.5$ for Cu–water.

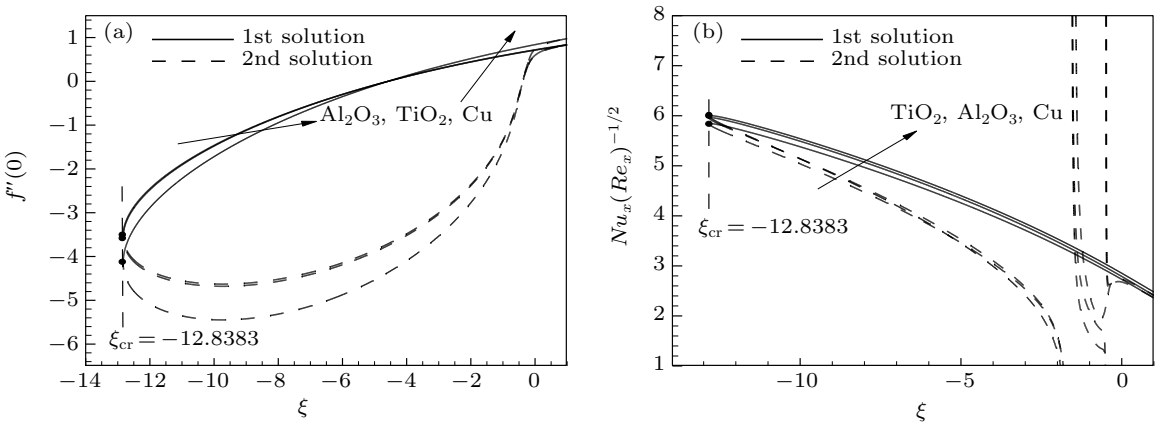


Fig. 3. $f''(0)$ (a) and $Nu_x Re_x^{-1/2}$ (b) as a function of ξ for different working fluids when $\phi = 0.1$, $\kappa = M = 0$, and $\varepsilon = 0.5$.

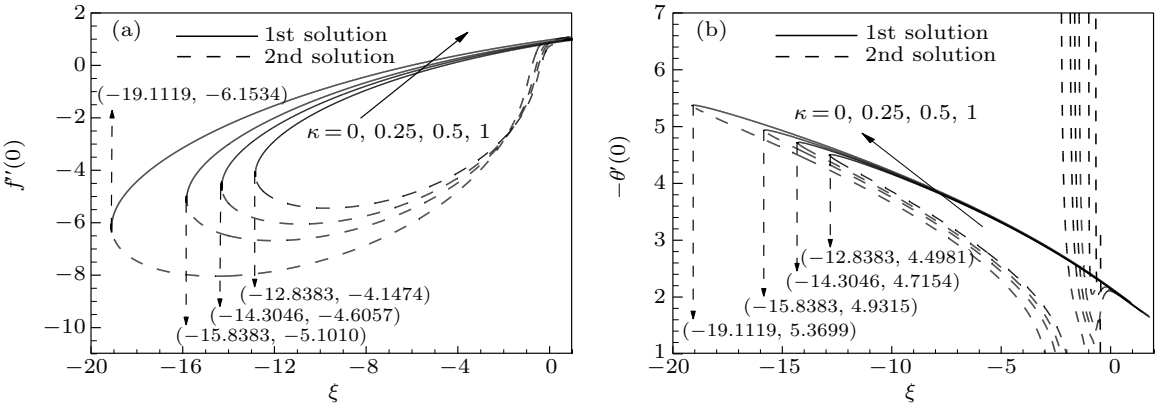


Fig. 4. $f''(0)$ (a) and $-\theta'(0)$ (b) as a function of ξ for different values of κ when $\phi = 0.1$, $M = 0$, and $\varepsilon = 0.5$ for Cu–water.

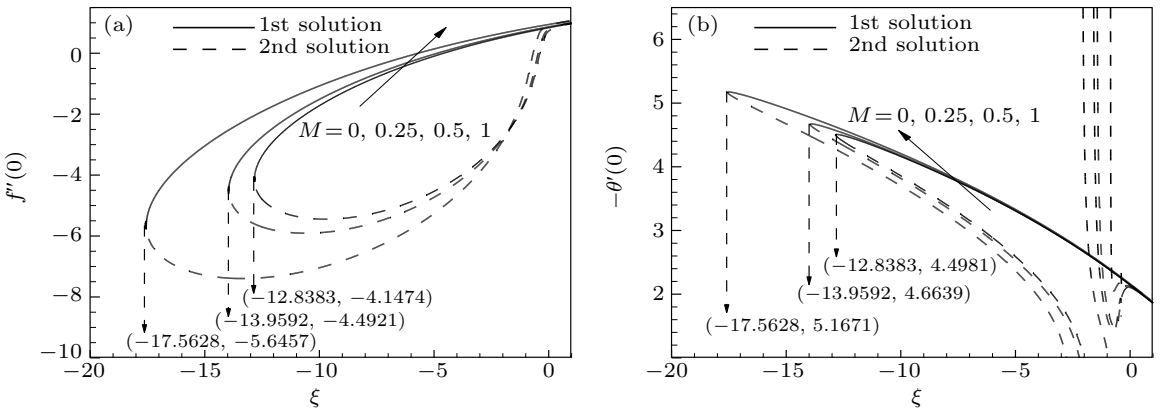


Fig. 5. $f''(0)$ (a) and $-\theta'(0)$ (b) as a function of ξ for different values of M when $\phi = 0.1$, $\kappa = 0$, and $\varepsilon = 0.5$ for Cu–water.

Figure 6 illustrates the variations of $f''(0)$ and $-\theta'(0)$ with ξ for different values of velocity ratio ε. It is seen that the solution domain increases with the increase of ε. Figure 7 shows a comparison between the effects of magnetic parameter and permeability parameter on the nanofluid flow and heat transfer for Cu–water working fluid with $\phi = 0.1$. It shows that for a stretching sheet ($\varepsilon = 0.5$) and equal values of M and κ, permeability parameter has a greater effect on the skin friction coefficient and the Nusselt number. Furthermore, the solution domain increases with the increases of M and κ. Table 4 presents some values of ε_{cr} and corresponding values of $f''(0)$ and $\theta'(0)$ for different values of κ, M, and ϕ when $\xi = -1$ for Cu–water. It is found that the value of $|\varepsilon_{cr}|$ increases with the increase of M or κ, thus the presence of magnetic field as well as porous medium increases the range of ε for which the solution exists.

Table 4. The values of ε_{cr} for different values of κ, M, and ϕ when $\xi = -1$ for Cu–water.

ϕ		$M = 0$		$\kappa = 0$	
		$\kappa = 0$	$\kappa = 0.25$	$M = 0$	$M = 0.25$
0	ε_{cr}	−0.75177	−0.93606	−0.75177	−0.93606
	$f''(0)$	0.147235	0.262175	0.147235	0.262175
	$\theta'(0)$	2.577431	5.880173	2.577431	5.880173
0.1	ε_{cr}	−0.75177	−0.88472	−0.75177	−0.85365
	$f''(0)$	0.172964	0.26859	0.172964	0.250021
	$\theta'(0)$	0.937695	1.591946	0.937695	1.420454
0.2	ε_{cr}	−0.75177	−0.87533	−0.75177	−0.82217
	$f''(0)$	0.179338	0.264586	0.179338	0.233196
	$\theta'(0)$	0.472890	0.835968	0.472890	0.653755

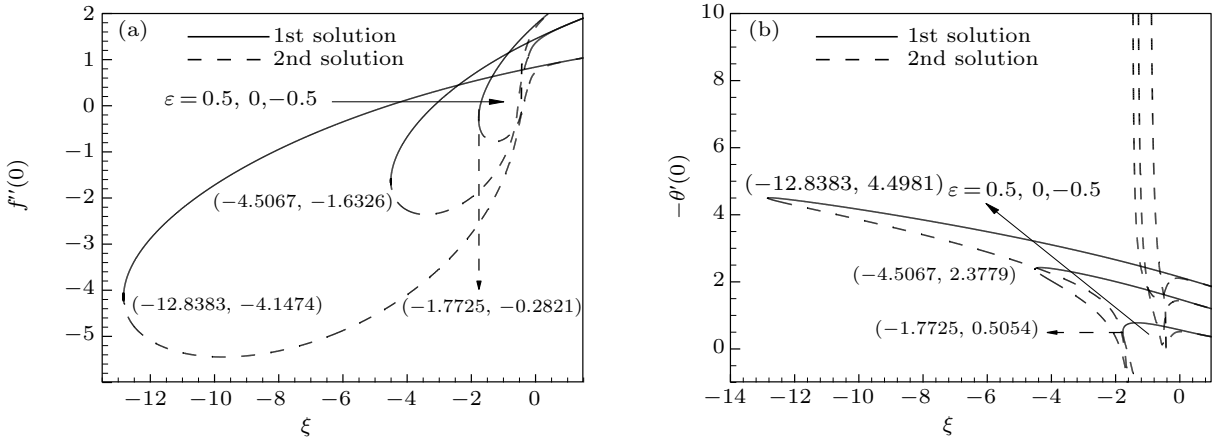


Fig. 6. $f''(0)$ (a) and $-\theta'(0)$ (b) as a function of ξ for different values of ε when $M = \kappa = 0$, and $\phi = 0.1$ for Cu–water.

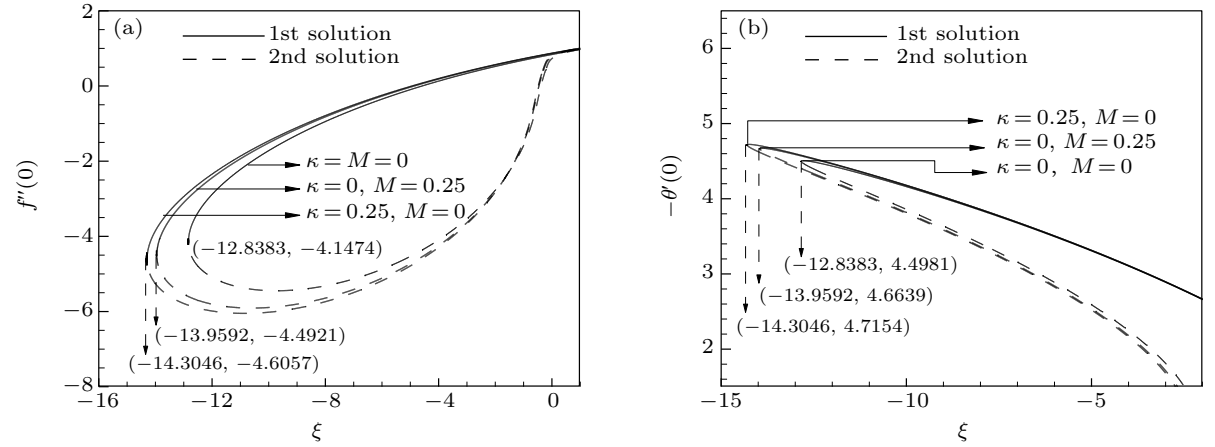


Fig. 7. Comparision between effect of M and κ on $f''(0)$ (a) and $-\theta'(0)$ (b) when $\varepsilon = 0.5$, $\phi = 0.1$ for Cu–water.

The samples of velocity and temperature profiles are presented in Figs. 8 and 9. These figures show that the boundary conditions (9) are satisfied and approach infinity asymptotically, which exhibits the existence of the dual solution. In Fig. 8, as expected, the magnitudes of the velocity and temperature gradient at the surface increase as the solid volume fraction of the nanofluid ϕ increases. Figure 9 shows that for a shrinking sheet ($\varepsilon = -0.5$) and equal values of M and κ, the permeability parameter has a greater effect on the skin friction coefficient and the Nusselt number, while a similar behavior is observed for the stretching sheet in Fig. 7. Further, figure 8(a) shows that in the second solution profiles, there are regions where $f' < -0.5$. Because of the negative pressure gradient in the x direction, this behavior is not physically realizable. A similar behavior is observed in Fig. 9(a).

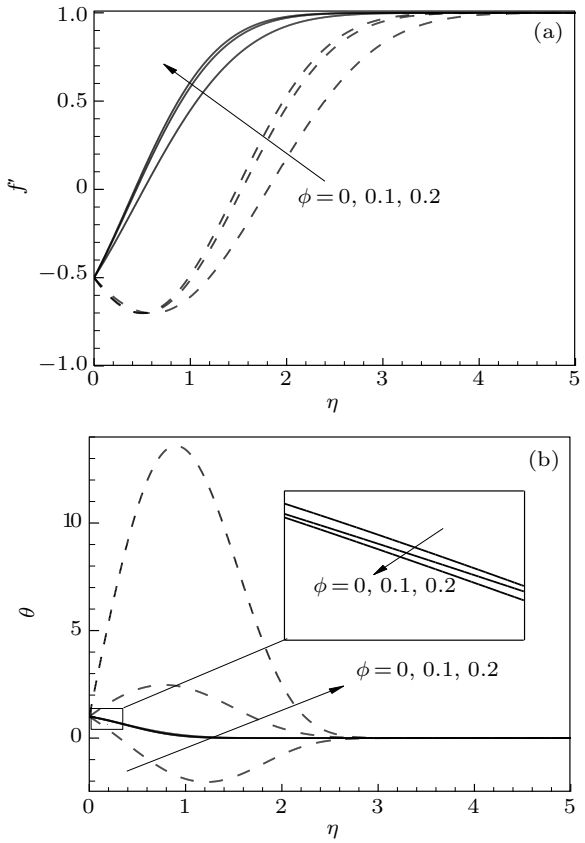


Fig. 8. Velocity (a) and temperature (b) profiles for different values of ϕ when $\varepsilon = -0.5$, $\xi = -1$, and $\kappa = M = 0$ for Cu–water.

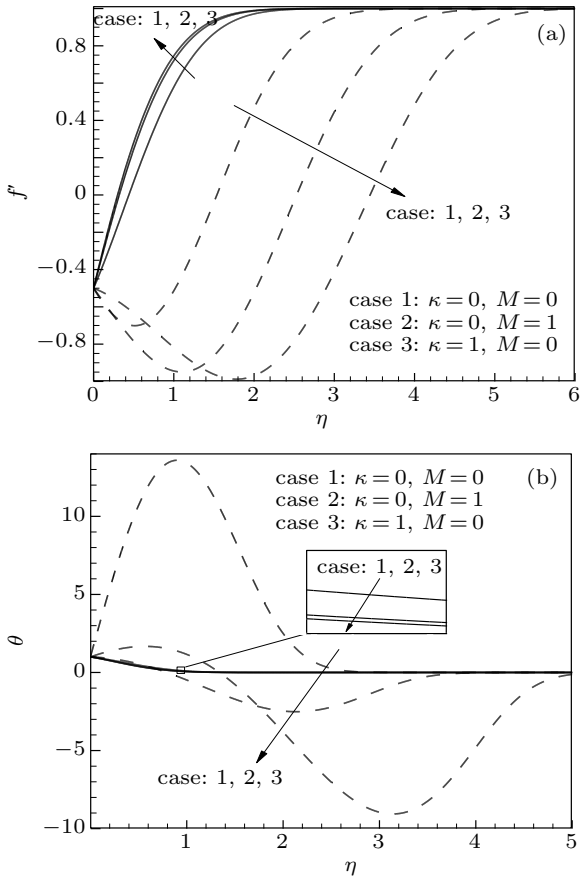


Fig. 9. Comparison effects of M and κ on velocity (a) and temperature (b) profiles when $\varepsilon = -0.5$, $\xi = -1$, and $\phi = 0.1$ for Cu–water.

4. Conclusions

We studied the similarity solutions of the unsteady MHD stagnation point flow and heat transfer of a nanofluid adjacent to a linearly stretching/shrinking sheet in a porous medium. The obtained similarity ordinary differential equations are solved using the fourth-order Runge–Kutta method with shooting technique. We discuss the effects of the governing parameters ξ, ε, ϕ, κ, M, and the type of nanoparticle on the fluid flow and heat transfer characteristics. Dual solutions are found for the boundary layer equations for decelerated flow ($\xi < 0$). It is seen that the skin friction and heat transfer coefficients increase with the increase of the nanoparticle volume fraction parameter ϕ. For equal values of M and κ, the permeability parameter has greater effects on the skin friction coefficient and the Nusselt number, whereas there is no difference between effects of these parameters for an ordinary fluid. Furthermore, it is found that the value of $|\xi_{\rm cr}|$ increases with the increase of M or κ, thus the presence of magnetic field as well as porous medium increases the range of ξ for which the solution exists. According to the above discussion, we can control the fluid flow and heat transfer by changing various parameters such as ξ, ε, ϕ, κ, M, and the type of nanoparticle. The study of nanofluids is still at its early stage, so that complementary works are necessary to understand the flow and heat transfer characteristics of nanofluids.

References

[1] Moore F K (NACA) TN-2471[1951-9]
[2] Lin C C 1956 *Proc. 9th Int. Congr. Appl. Mech.*, September 5–13, 1956, Brussels, Belgium, p. 155
[3] Wang C Y 1990 *Q. Appl. Math.* **48** 601
[4] Bachok N, Ishak A and Pop I 2012 *Int. J. Heat Mass Transfer* **55** 2102
[5] Suali M, Nik Long N M A and Ariffin N M 2012 *J. Appl. Math.* **2012**
[6] Fang T G, Zhang J and Zhong Y F 2011 *Chin. Phys. Lett.* **28** 124707
[7] Rohni A M, Ahmad S and Pop I 2012 *Int. J. Heat Mass Transfer* **55** 1888
[8] Shahzad A, Ali R and Khan M 2012 *Chin. Phys. Lett.* **29** 084705
[9] Wang C Y 2008 *Int. J. Non-Linear Mech.* **43** 377
[10] Dinarvand S, Hosseini R, Damangir E and Pop I 2013 *Meccanica* **48** 643
[11] Kamali R and Binesh A R 2010 *Int. Commun. Heat Mass Transfer* **37** 1153
[12] Choi S U S 1995 *IMECE*, Novamber 12–17, 1995, San Francisco, USA p. 99
[13] Khanafer K, Vafai K and Lightstone M 2003 *Int. J. Heat Mass Transfer* **46** 3639
[14] Tiwari R J and Das M K 2007 *Int. J. Heat Mass Transfer* **50** 2002
[15] Oztop H F and Abu-Nada E 2008 *Int. J. Heat Fluid Flow* **29** 1326
[16] Zhou X F and Gao L 2007 *Chin. Phys.* **16** 2028
[17] Tamim H, Dinarvand S, Hosseini R, Khalili S and Pop I 2013 *Proc. Inst. Mech. Eng. E J. Process Mech. Eng.* (published online)
[18] Dinarvand S, Abbassi A, Hosseini R and Pop I 2012 *Thermal Science*, first issue, p. 165
[19] Khalili S, Khalili A, Kafashian S and Abbassi A 2013 *J. Porous Media* **16** 967
[20] Das S K, Choi S U S, Yu W and Pradeep T 2007 *Nanofluids: Science and Technology* (New Jersey: John Wiley & Sons) p. 1
[21] Kakacç S and Pramuanjaroenkij A 2009 *Int. J. Heat Mass Transfer* **52** 3187
[22] Eagen J, Rusconi R, Piazza R and Yip S 2010 *ASME J. Heat Transfer* **132** 102402

[23] Lee J H, Lee S H, Choi C J, Jang S P and Choi S U S 2010 *Int. J. Micro-Nano Scale Transport* **1** 269
[24] Fan J and Wang L 2011 *ASME J. Heat Transfer* **133** 040801
[25] Takhar H S and Ram P C 1994 *Int. Commun. Heat Mass Transfer* **21** 371
[26] Raptis A, Massalas C and Tzivanidis G 1982 *Phys. Lett. A* **90** 288
[27] Fang T and Zhang J 2009 *Commun. Nonlinear. Sci. Numer. Simul.* **14** 2853
[28] Fang T G, Zhang J and Yao S S 2010 *Chin. Phys. Lett.* **27** 4702
[29] Khalili S, Dinarvand S, Hosseini R, Saber M and Pop I 2013 *Proc. Inst. Mech. Eng. E J. Process Mech. Eng.* (in press)
[30] Nakayama A 1995 *PC-Aided Numerical Heat Transfer and Convective Flow* (Tokyo: CRC Press) p. 1
[31] Nield D A and Bejan A 2013 *Convection in Porous Media*, 4th edn. (New York: Springer) p. 1
[32] Ingham D B and Pop I 1998 *Transport Phenomena in Porous Media* (Oxford: Pergamon Press) p. 1
[33] Bachok N, Ishak A and Pop I 2012 *Int. J. Heat Mass Transfer* **55** 6499
[34] Brinkman H C 1952 *J. Chem. Phys.* **20** 571
[35] Postelnicu A and Pop I 2011 *Appl. Math. Comput.* **217** 4359
[36] Roşca A V and Pop I 2013 *Int. J. Heat Mass Transfer* **60** 355